*Journal of Natural Disaster Science, Volume 24, Number 2, 2002, pp101-107*

# Health Monitoring Algorithm by the Monte Carlo Filter Based on Non-Gaussian Noise

Ikumasa YOSHIDA
Tokyo Electric Power Services Co.,Ldt., Tokyo, Japan
Tadanobu SATO
Disaster Prevention Research Institute, Kyoto University, Kyoto, Japan

(Received for 4 Mar., 2002)

**ABSTRACT**

A basic study of the application of the Monte Carlo filter (MCF) to structural damage detection is reported. In that method, each probability distribution is expressed by many of its realizations, called particles or samples. The advantage of the MCF is that it deals with non-linear and non-Gaussian problems. In terms of damage detection, non-Gaussian noise may be preferable because the damage tends to be concentrated on a specific part of a structure. Two kinds of numerical examples are shown. First, the stiffness of the experimental model for the shaking table test is identified by the MCF and EKF (Extended Kalman Filter). Based on hypothetical data, numerical simulations of damage detection with non-Gaussian process noise then are performed and discussed. Because the MCF results are given by many particles (samples), the detailed probabilistic nature of the identified parameters also can be discussed.

## 1. INTRODUCTION

After a large earthquake, rapid detection of damage to structures, especially important ones such as hospitals, bridges, fire stations, is needed to prevent secondary disasters. Extensive time and costs are involved in estimating damage to such structures visually, if inspected in detail, the conventional way. Recently, many important structures are being monitored with sensors such as seismometers. A practical method for rapid detection of damage to the structures that uses monitored data is desirable from the standpoint of damage detection or health monitoring.

Linear/Nonlinear identification methodology has been well studied. Of the various reported methods, the Kalman filter is one of the best known and widely used algorithm owing to its beautiful, sophisticated theory which requires only the first and second moment of probabilistic nature because the filter is well established on the basis of linear Gaussian assumptions. In the field of structural identification, the Kalman filter has been one of the most widely used tools (Yun & Shinozuka 1980, Hoshiya & Saito 1984). Although various nonlinear identification methods have been proposed, most have the same limitation as the Kalman filter as they are based on Gaussian noise, leading to the quadratic form of the objective function.

Structural damage must be non-stationary phenomenon, therefore process noise has an important function because it works as a forgetting factor (Koh & See 1994, Hoshiya & Yoshida 1998, Sato & kaji 2001). Although Gaussian process noise is used in the Kalman filter, other types of noise may be preferable for damage detection when the nature of the damaged structure is considered. Minor damage caused by seismic forces tends to be localized; e.g., it tends to be concentrated on a specific part of a structure. When a large destructive earthquake hits, damage will occur in many parts of a structure simultaneously. Cautious inspections of structures with such major damage is not required because the severity of the damage is clear. In damage detection, the assessment of minor to moderate damage is important. To detect such damage, Gaussian process noise, which derives the quadratic form of objective function, may not be appropriate.

Non-Gaussian identification methods are being investigated (Kitagawa 1996). Basically, the non-Gaussian approach requires much computation but because of remarkable advances in computer performance, new approaches that use the Monte Carlo technique have become practical; e.g., the Genetic Algorithm. The Monte Carlo Filter proposed by Kitagawa (1996) is a Monte Carlo method that deals with non-Gaussian noises. In it, probability distributions are approximated by many of their realizations; i.e., the many particles or samples. The probabilistic nature of a state vector is expressed by the many particles instead by the first and second moment as in the Kalman filter. A method of damage detection that uses the Monte Carlo filter is here proposed and demonstrated. Formulation of identification by means of Monte Carlo filter first is presented. It is the natural extension of the Kalman filter (linear Gaussian) but essentially a different method in that it is not necessary to use Gaussian noise. Two kinds of numerical examples are shown; identification of the stiffness of the experimental model for the shaking table test as reported by Loh (2000), performed by MCF and ordinary EKF (Extended Kalman filter), and numerical simulation of damage detection by the MCF with Gaussian or non-Gaussian process noise based on hypothetical data.

KEY WORDS: damage detection, health monitoring, state space, non-Gaussian filter

## 2. METHODOLOGY

### 2.1 The Kalman and Monte Carlo Filters

The general form of the state space model, including the non-linear state/observation equation and non-Gaussian noise, is described as follows. The state equation is

$$\boldsymbol{x}_k = \boldsymbol{F}(\boldsymbol{x}_{k-1}, \boldsymbol{w}_k) \tag{1}$$

where, $\boldsymbol{x}_k$ is the state vector at the k-th step, and $w_k$ the process noise. The observation equation is

$$\boldsymbol{y}_k = \boldsymbol{H}(\boldsymbol{x}_k, \boldsymbol{v}_k) \tag{2}$$

where, $\boldsymbol{y}_k$ is the observation vector at the $k$-th step, and $\boldsymbol{v}_k$ the observation noise. When the state and observation equations are linear, and the noises Gaussian, the Kalman filter technique, simple, very sophisticated filtering method, is applicable. The algorithm is presented in Fig. 1, where $\boldsymbol{Q}$ and $\boldsymbol{R}$ respectively represent the covariance matrix of $\boldsymbol{w}_k$ and $\boldsymbol{v}_k$. The probability distribution of a state vector is described solely by the first and second moments. The Kalman filter algorithm has two parts, a time-updating process and an observation-updating process. The time-updating process is a one-step ahead prediction based on the information at the ($k$-$1$)-th step. The predicted state vector and its covariance matrix are denoted as $\boldsymbol{x}_{k/k-1}$ and $\boldsymbol{P}_{k/k-1}$. The observation-updating process consists of the estimation based on observation data $\boldsymbol{y}_k$ at the $k$-th step and information predicted by the time-updating process. The estimated state vector and its covariance matrix are given as $\boldsymbol{x}_{k/k}$ and $\boldsymbol{P}_{k/k}$.

Several methods have been proposed for general, non-linear, and non-Gaussian problems, in which the probability function is approximated by a group of step functions, linear segments, or Gaussian distributions (Kitagawa 1996). These methods basically are limited to low dimensional problems because of the impracticality of extensive computation time when the dimension is large. In the Monte Carlo filter technique, probability functions are approximated by many of their realizations; i.e., particles or samples. The algorithm of MCF also is shown in Fig. 1. Its general flow is similar to that of the Kalman filter, but in the MCF the probabilistic nature of the state vector is described by many realizations instead of the first and second moments. The most important point of the MCF is the resampling in the observation updating process. The likelihood of each sample realization with respect to observation noise first is calculated. Next, the samples are resampled according to their likelihood ratios. Samples of large likelihood may be resampled several times, whereas samples of small likelihood may not be resampled at all.

### 2.2 State Transfer and Observation Equations for Damage Detection

The Monte Carlo filter algorithm is applied to structural damage detection problems. The equation of motion is given by

$$\boldsymbol{M}\ddot{\boldsymbol{u}}_r + \boldsymbol{C}\dot{\boldsymbol{u}}_r + \boldsymbol{K}\boldsymbol{u}_r = -\boldsymbol{M}\boldsymbol{h}\ddot{z} \tag{3}$$

where, $\boldsymbol{M}$, $\boldsymbol{C}$, and $\boldsymbol{K}$ represent the mass, damping, and stiffness matrix respectively and $\ddot{\boldsymbol{u}}_r$, $\dot{\boldsymbol{u}}_r$ and $\boldsymbol{u}_r$ the relative acceleration, velocity, and displacement to the input motion. The notation $\ddot{z}$ represents input acceleration, and $\boldsymbol{h}$ is a vector whose components are unity ( $\boldsymbol{h} = (1,1,1,\ldots,1)^T$ ).

Two types of formulation are introduced. The first, proposed by Sato & Kaji (2000), is called Type-1 in this paper. The state vector, $\boldsymbol{x}$, is composed simply of unknown parameters such as stiffness and the damping ratio. The state equation is given by the simple form.

$$\boldsymbol{x}_k = \boldsymbol{x}_{k-1} + \boldsymbol{w}_k \tag{4}$$

The observation equation is

$$\boldsymbol{y}_k = \boldsymbol{H}_k \boldsymbol{x}_k + \boldsymbol{v}_k = -\boldsymbol{M}^{-1}\boldsymbol{C}_k\dot{\boldsymbol{u}}_r - \boldsymbol{M}^{-1}\boldsymbol{K}_k\boldsymbol{u}_r - \boldsymbol{h}\ddot{z} + \boldsymbol{v}_k \tag{5}$$

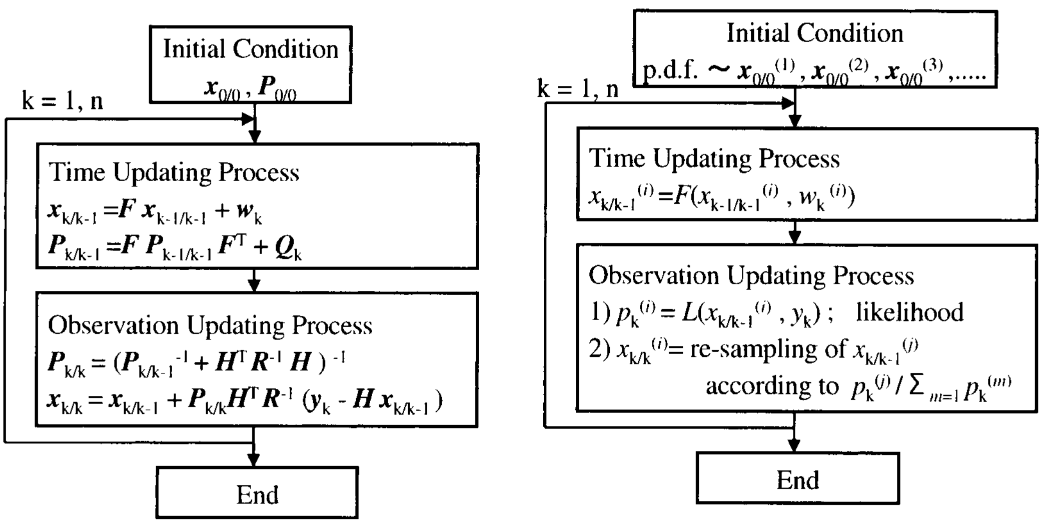


(a) (b)

Fig. 1 Time-updating and observation-updating processes of the filtering algorithms. (a) Kalman filter; (b) Monte Carlo filter

In this formulation, the observation vector, $\boldsymbol{y}_k$, represents the response accelerations of all the nodes. Velocity and displacement of all the nodes also are necessary on the right side of Equation (5). The equation of motion is considered in the observation equation, in which the state vector $\boldsymbol{x}_k$ contains $\boldsymbol{C}_k$ and $\boldsymbol{K}_k$. As both Equations (4)(5) are linear, the Kalman filter is applicable when the noises $\boldsymbol{w}_k$ and $\boldsymbol{v}_k$ are Gaussian. The advantage of the Type-1 formulation is that it is simple and practical, whereas the disadvantage is that it needs motions of all degrees of freedom as observation data.

In the Type-2 formulation, the state vector x is composed of the motions of all the nodes and unknown parameters;

$$x = \begin{pmatrix} x_a \\ x_b \end{pmatrix} \quad x_a = \begin{pmatrix} \ddot{u}_r \\ \dot{u}_r \\ u_r \end{pmatrix} \tag{6}$$

where $\boldsymbol{x}_b$ represents unknown parameters. The state equation is

$$\boldsymbol{x}_{a,k} = \boldsymbol{F}(\boldsymbol{x}_{a,k-1}, \boldsymbol{x}_{b,k}) + \boldsymbol{w}_{a,k} \tag{7a}$$

$$\boldsymbol{x}_{b,k} = \boldsymbol{x}_{b,k-1} + \boldsymbol{w}_{b,k} \tag{7b}$$

where $\boldsymbol{F}(\boldsymbol{x})$ is the function that represents one-step prediction. The equation of motion is considered in the function, $\boldsymbol{F}(\boldsymbol{x})$. In the following numerical examples, the linear acceleration method was used for $\boldsymbol{F}(\boldsymbol{x})$. The observation equation is written simply;

$$\boldsymbol{y}_k = \boldsymbol{H}\boldsymbol{x}_k + \boldsymbol{v}_k \tag{8}$$

where $\boldsymbol{H}$ is a constant simple matrix which indicates observation point locations. In this formulation, identification with observed data of part of the nodes can be performed theoretically. Only the Type-2 formulation is discussed in the following numerical examples.

## 2.3 Type of Noises

In the state space model, process noise has an important role. The probability density functions of Pearson's family are shown in Fig. 2. The Cauchy, Student's t, and Gausssian distributions are family members. The Cauchy and Gausssian distributions have opposite characteristics. The central part of the Gaussian distribution is the thickest, whereas that of the Cauchy distribution is the thinnest, indicative that the tail part of the Cauchy distribution is the heaviest. The distribution with heavier tail part than that of the Cauchy distribution is proposed. It is a combination of the delta function and uniform distribution. This distribution is illustrated in Fig. 2(b). This distribution here is called the U-D (Uniform-Delta) distribution.

Gaussian noise is interpreted as having L2-norm (Menke 1989) from its quadratic form of the objective function (penalty

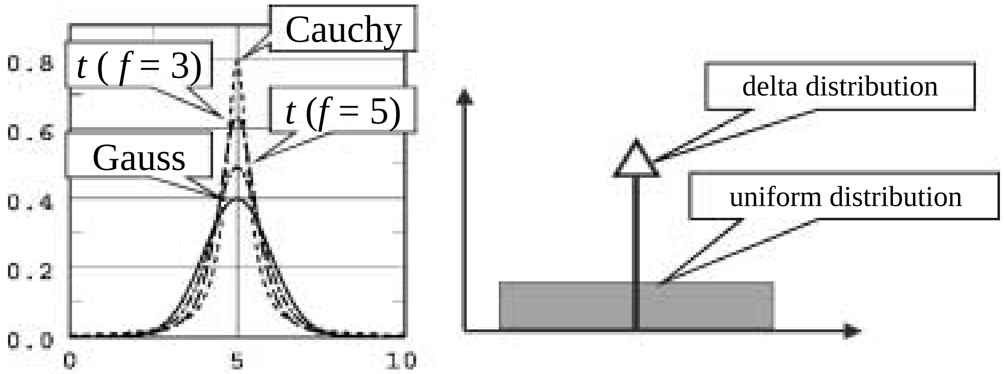


(a) (b)

Fig. 2 Probability Density Functions. (a) Pearson's family probability density functions, Cauchy, Student's t (f : degree of freedom), Gaussian distribution; (b) Uniform-Delta (U-D) distribution

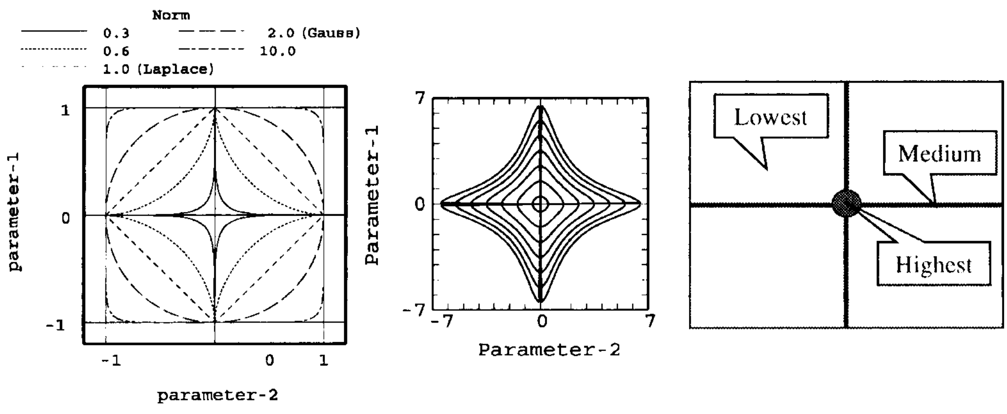


(a) (b) (c)

Fig. 3 Contour map shapes of probability density functions. (a) Norms of several types of probability density function; (b) Cauchy distribution; (c)Uniform and Delta distribution (U-D) function, cost functions). This means that distance is defined as in our physical world. Fig. 3 shows contour map shapes of three types of probability density functions in two-dimensional space. The Gaussian shape is a circle (ellipse), whereas that of the Laplace distribution is a square, interpreted as having the L1-norm. The shape of the Cauchy contour depends on the part of the probability density function. The shape of the contour map is almost a circle near the origin (mean), evidence that the norm is close to L2, but at the tail part the norm seems to be lower. The shape of the U-D distribution is very simple, having only three levels of height in two dimensional space. The highest part is at the mean point (origin), the second highest on the axes, and the other parts are the lowest. The shape of this probability density function also suggests a very low norm.

The type of probability density function determines the form of the objective function for identification and has a significant effect on the estimated parameters. Identification made with low norm noise tends to identify concentrated damage to a specific part of a structure as compared with identification made with higher norm noises. In fact, however, minor to moderate damage caused by seismic forces tends to be localized, i.e., it tends to be concentrated. This suggests that lower norm noises are better for the purpose of damage detection, although Gaussian noises are widely used. In the following numerical examples, Gaussian and U-D noises are compared.

## 3. NUMERICAL EXAMPLES

### 3.1 Identification with experimental data

The experimental data of Loh (2000) was used to identify the stiffness of the model by two methods, Extended Kalman (EKF) and Monte Carlo (MCF) filters described earlier. Fig. 4 shows a sketch of the experimental model as well as the response accelerations on the top floor and on the shaking table. A model of a five-story steel structure is installed on the shaking table. The height of the model is 650cm. Many sensors, acceleration meters, velocity meters, and strain gauges are attached to the model. Shaking tests were carried out under various conditions to obtain a set of earthquake response data. In this numerical study, data observed under the following excitation conditions were used.

- Earthquake: Kobe (1995, meteorological observatory, vertical to fault component)
- Scale for input motion: 48%

The type-2 formulation of the structural identification, given earlier was used for both the MCF and EKF methods. The formulation for the EKF is essentially that proposed by Hoshiya & Saito (1984). The purpose of the identification is for estimation of the stiffness of the model, not for damage detection, therefore Gaussian process noise also was used in the MCF. The particle

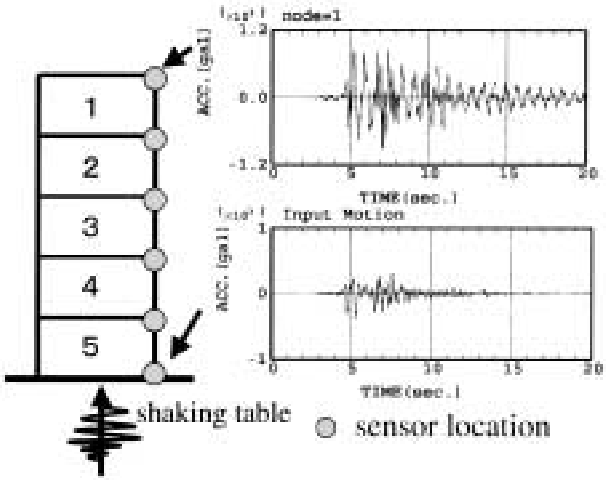


Fig. 4 Sketch of the experimental model and time histories of response accelerations

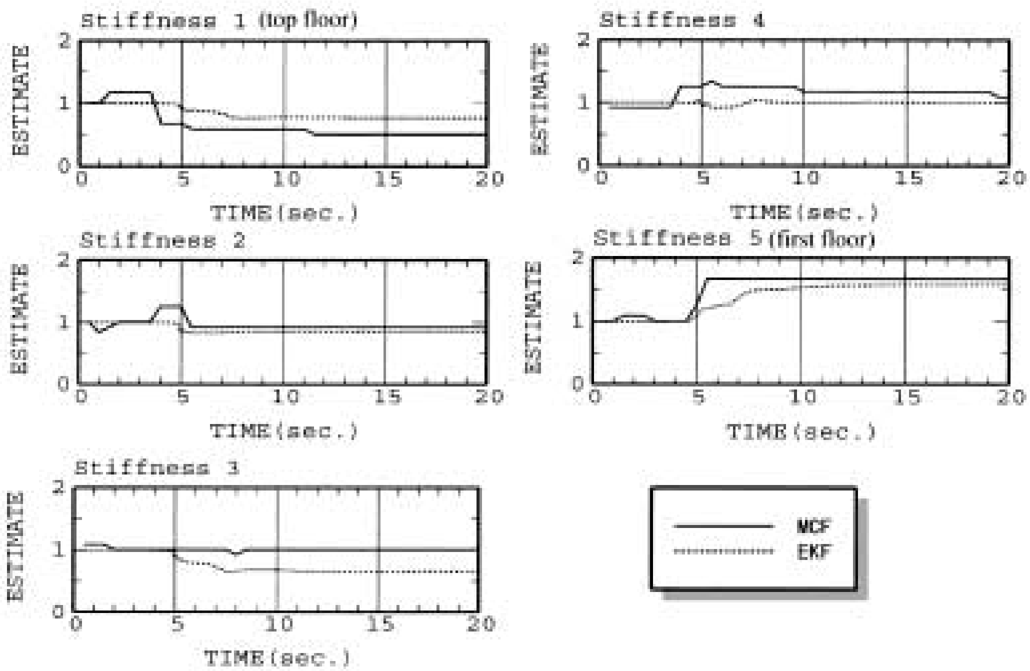


Fig. 5 Identified stiffnessess of the experimental model by the MCF (Monte Carlo filter) and EKF (Extended Kalman filter) methods

(sample) number was 1000. In the EKF, no process noise was considered. As no data on mass distribution was available, uniform mass distribution is assumed. Initial stiffness values were determined based on the 1st predominant frequency of the Fourier spectral ratio of response at the top floor to the motion of the shaking table.

The observed data for all the floors were used for the identification. The time histories of the identified stiffness are shown in Fig. 5 as ratios to the initial value. Although the same stiffness values are not identified by the two methods, the trend is the same. The identified stiffness of the upper parts, especially the top floor, is smaller than that of lower parts.

Identifications based on observed data for a specific floor also were tried, but no stable solutions were obtained. The identified stiffness varied depending on the observation point. When the EKF was used, solutions sometimes were not obtained due to numerical explosion. When the MCF was used, numerical explosions did not occur because the parameter ranges are defined, but the solutions obtained also were not stable. Identifications made with observation data for two specific floors also were tried. More stable solutions were obtained, but solutions still sometimes became unstable.

### 3.2 Damage detection with hypothetical data

In this numerical example, the hypothetical 5-DOF model, shown in Fig. 6, was used. All the elements (floors) have the same weight, initial stiffness, and initial damping ratio; respectively 9.8tf/m3, 400 tf/m2, and 0.02. Damage is assumed to occur at element 3, where stiffness decreases from 400 to 360 tf/m2 and the damping ratio increases from 0.02 to 0.04 during 6-7 seconds. Due to this damage, the fundamental frequency of the model is reduced, from 1.0 to 0.99Hz.

The input and response motions for nodes 1 and 3 are shown in Fig. 7. The observation data obtained for damage detection add 3% (rms ratio) Gaussian white noises to the response data. The number of particles is 1000. Identification for up to 10000 particles was tried, but the performance was almost the same. For fewer than 1000 particles, however, the performance was bad. When the SODF simulation was tried, good results were obtained even for a particle number of 100.

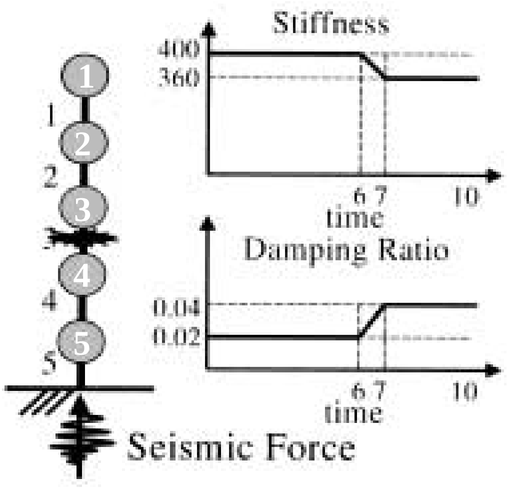


Fig. 6 Hypothetical 5-DOF model with damage to element 3

Damage detection by the MCF can be done under various conditions. Results of the cases shown in Table 1 are here discussed. In all of them, the Cauchy distribution was used for the observation noise. First, cases 1 and 2 results are discussed, in which the U-D distribution was used as the process noise. The particle distributions of the estimated stiffness and damping ratio of element 3 are shown respectively in Figs. 8 and 9. These figures are considered to show the non-stationary probability density function of the identified parameters. When data for all the nodes was used, the stiffness distribution peak was clear as shown (Fig. 8). When the observation data was limited to nodes 1 and 3, the distribution peak was not as clear (Fig. 9), but the trend for the stiffness distribution peak to moves after about 6 seconds is still clear. The trend of the damping ratio is observable, but generally is not clear. Although many simulations under various conditions were tried, identification of the change in the damping ratio was very difficult. Because the identified damping ratios are very unstable, the discussion hereafter concentrates on stiffness.

Estimator needs to be determined from the particle distributions for practical damage detection. The most popular estimator is the mean, which sometimes is inadequate. The histograms in Fig. 10 represent the identified stiffness distributions of element 3 at 6 and 9 seconds in case 2, which corresponds to the time sections in Fig. 9. A single distribution peak is presented at 6 sec-

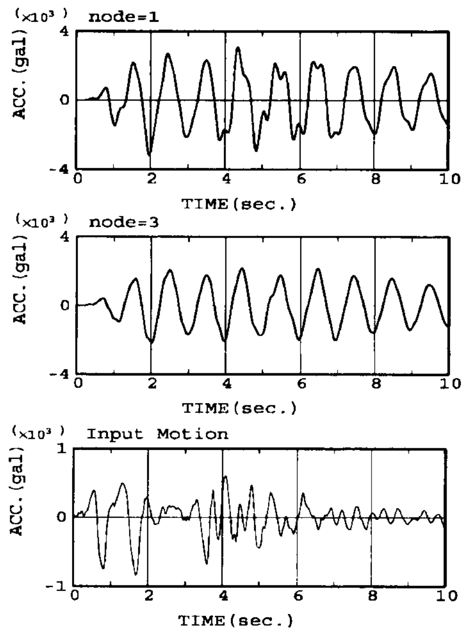


Fig. 7 Acceleration time histories of input motion and responses

Table 1. Numerical calculation cases

| case | observation | process noise |
|---|---|---|
| 1 | all | U-D* |
| 2 | nodes 1 & 3 | U-D* |
| 3 | all | Gaussian |
| 4 | nodes 1 & 3 | Gaussian |

U-D* : uniform and delta distribution

onds, and the mean, median, and mode of distribution appear to be almost the same. At 9 seconds, however, there are three peaks, and the distribution shape is not symmetric. The mean value therefore may not be an appropriate estimator. Interestingly, the highest peak is close to the true damage stiffness, and the second highest one is close to the initial value. In this study, we used the highest distribution peak, the mode of particles as the estimator.

The identified stiffnesses (highest distribution peak, mode) of elements 2, 3, and 4 are shown in Fig. 11. When observation data for all the nodes were used, damage was detected properly despite the type of process noise. The identified stiffnesses of 2 and 4 are almost constant, but the stiffness of 3 decreases after 6 seconds. When the observed data were limited to nodes 1 and 3, U-D process noise seemed to be better than Gaussian process noise in this numerical simulation. These results suggest that the MCF with non-Gaussian process noise is appropriate to use for damage detection. The advantage using the U-D process noise could not be definitively shown because the identified parameters are sensitive to numerical conditions. Further studies on the modeling/tuning of process noise and a more stable algorithm are needed.

## 4. CONCLUSIONS

Formulation of damage detection by means of the Monte Carlo filter was introduced and the validity of that method demonstrated for two types of numerical simulations. The conclusions are as follows;

1) Formulation of damage detection by the Monte Carlo filter (MCF) is possible. The U-D distribution for which the norm is very low, also can be used for damage detection.
2) Parameter identification in the experimental model can be maded by the MCF and ordinary Extended Kalman filter

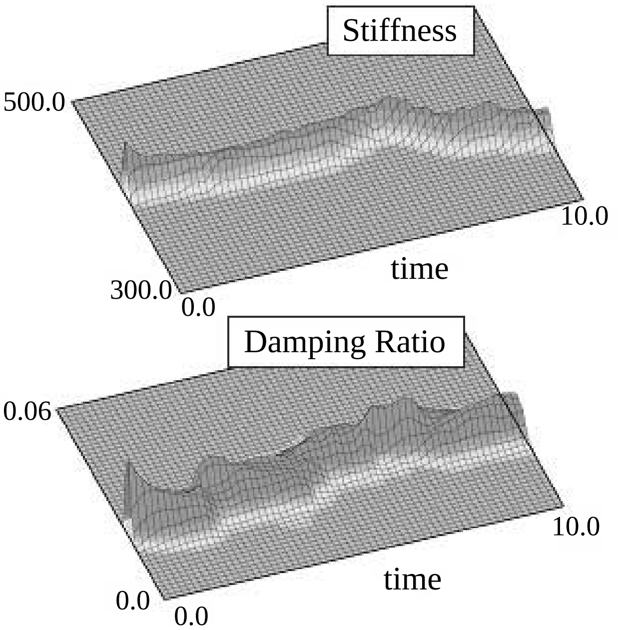


Fig. 8 Distribution of stiffness particles and the damping ratio of element 3
(case-1 observation data for all nodes, U-D Proc-ess Noise)

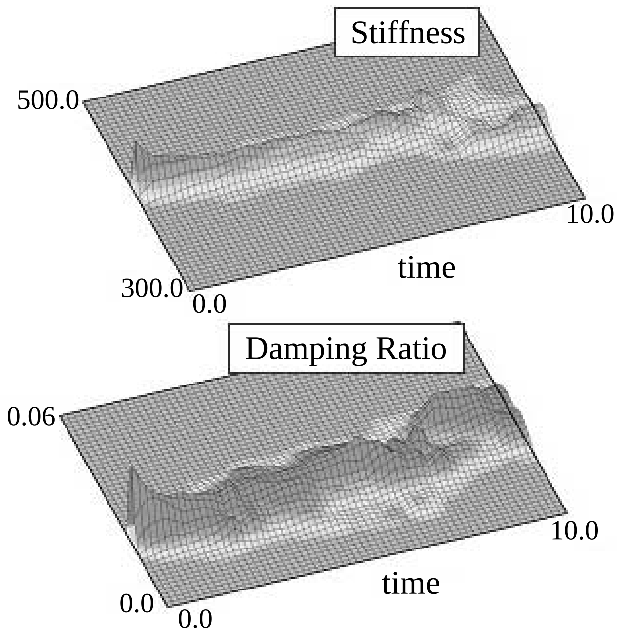


Fig. 9 Distribution of stiffness particles and the damping ratio of element 3
(case-2 observation data for nodes 1 and 3, U-D process noise)

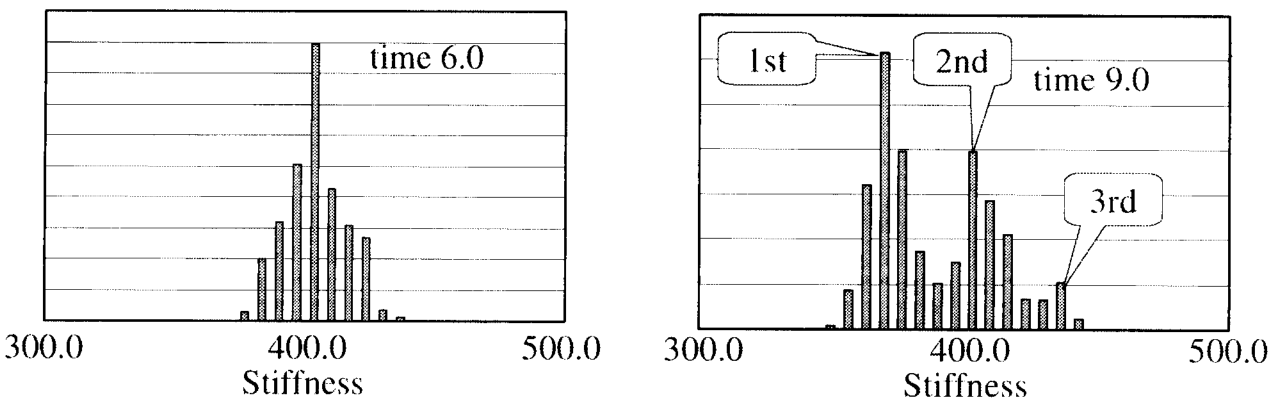


Fig. 10 Estimator of element 3 stiffness based on the particle distribution
(case-2 observation data for nodes 1 and 3, U-D process noise)

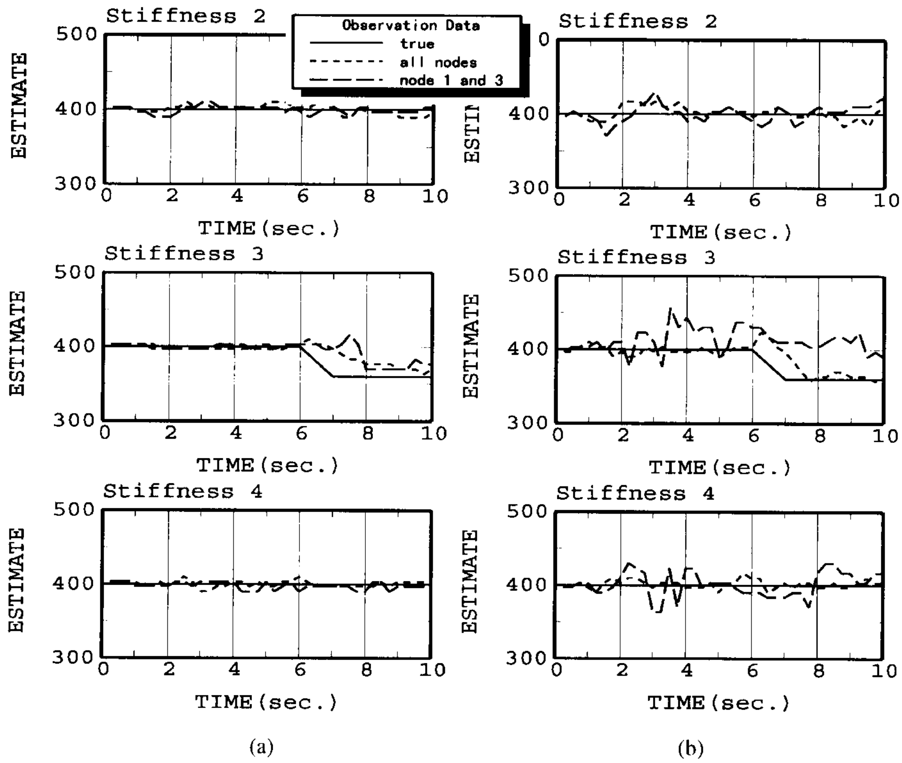


Fig. 11 Identified stiffnesses of elements 2, 3, and 4. (a) U-D process noise; (b) Gaussian process noise

(EKF) methods. Similar parameter trends are identified by both methods.

3) Damage detection by the MCF is done with Gaussian or U-D noise which has a very low norm in the objective function of identification. Numerical simulations findings suggest that the use of low norm process noise is suitable for damage detection problems.

In the MCF, the parameters identified sometimes vary depending on numerical conditions such as particle number, seed of random number, and noise parameters. Further improvements such as adaptive tuning, use of the proper type of process noise, and a more stable algorithm are needed for a practical tool. The MCF appears to be a prospective tool to detect damage done to a structure, because it is applicable to a broad range of non-linear and non-Gaussian problems.

## REFERENCES

Kitagawa, G.., 1996. Monte Carlo Filter and smoother for non-Gaussian state space models, Journal of Computational and Graphical Statistics, 5(1), 1-25.

Koh, C.G. and See, L.M., 1994. Identification and uncertainty estimation of structural parameters, ASCE Journal of Engineering Mechanics, 120(6), 1219-1236.

Loh, C.-H., 2000. The report o f shaking table test results and numerical simulation o f a five- story steel frame structure, NCREE Report, (in Chinese).

Menke, W., 1989. Geophysical data analysis: discrete inverse theory, Academic Press, Inc.

Hoshiya, M. and Saito, E., 1984. Structural identification by extended Kalman Filter, ASCE Journal of Engineering Mechanics, 110(12), 1757-1770.

Hoshiya, M. and Yoshida, I., 1998. Process noise and optimum observation in conditional stochastic fields, ASCE Journal of Engineering Mechanics, 124(12), 1325-1330

Tadanobu SATO, Kai QI. 1998. Adaptive H∞ filter: Its application to structural identification, ASCE Journal of Engineering Mechanics, 124(11), 1233-1240

Sato, T. and Kaji, K., 2001. Adaptive Monte Carlo filter and structure identification, Proceedings of the first International Conference on Monte Carlo Simulation, pp.441～pp.447

Yun, C.-B. and Shinozuka, M., 1980. Identification of nonlinear structural dynamic systems, ASCE Journal of Engineering Mechanics, 8(2), 187-203